

## Quark production and thermalization of the longitudinally boost-invariant quark-gluon plasma

---

**Sergio Barrera Cabodevila,<sup>a,\*</sup> Xiaojian Du,<sup>a</sup> Carlos A. Salgado<sup>a,b</sup> and Bin Wu<sup>a</sup>**

<sup>a</sup>*Instituto Galego de Física de Altas Enerxías IGFAE, Universidade de Santiago de Compostela, E-15782 Galicia, Spain*

<sup>b</sup>*Axencia Galega de Innovación (GAIN), Xunta de Galicia, Galicia, Spain*

*E-mail:* [sergio.barrera.cabodevila@usc.es](mailto:sergio.barrera.cabodevila@usc.es)

We use the Boltzmann Equation in Diffusion Approximation (BEDA) as a tool to explore the time evolution of an initially out-of-equilibrium and highly occupied expanding system of gluons. We study the hydrodynamization of this system as well as the quark production until chemical equilibration is established. A comprehensive study of such processes will be presented based on parametrical estimations in the weak-coupling limit, similar to those employed for bottom-up thermalization in pure gluon systems, as well as complementary numerical solutions of the BEDA. Our studies provide a better understanding of the underlying processes involved in the different stages of the evolution.

*42nd International Conference on High Energy Physics (ICHEP2024)  
18-24 July 2024  
Prague, Czech Republic*

---

\*Speaker

## 1. Introduction

After a heavy ion collision, a highly populated and non-equilibrated, quickly expanding system of gluons is produced. Combining this picture with the hydrodynamic description of the Quark Gluon Plasma (QGP) is one of the field's most intriguing phenomena, typically referred to as thermalization/hydrodynamization. In the weak coupling limit, this process follows a time evolution known as the "bottom-up thermalization" [1]. Understanding how this process is produced is critical if one attempts to comprehend the evolution in the small collision systems, where the medium might not be able to fully thermalize and, therefore, it would not exhibit all the features that have been proved in the heavy ion collisions.

The Color Glass Condensate formalism describes how this highly populated system of gluons is produced up to some time  $\tau \sim Q_s^{-1}$ , where the saturation momentum  $Q_s$ , is the typical momentum of the gluons produced right after the collision. We aim to describe the thermalization/hydrodynamization process for a longitudinally boost-invariant expanding plasma. This has been previously explored numerically in the Effective Kinetic Theory (EKT) [2–4]. In contrast, here we will use the Boltzmann Equation in Diffusion Approximation (BEDA) [5, 6] as an alternative framework, whose inelastic kernel coincides with that used in [1], and elastic kernel is more efficient to calculate. We generalize the BEDA for a longitudinally expanding plasma composed of quarks and gluons and study the parametric features in comparison to the numerical results.

## 2. The Boltzmann Equation in Diffusion Approximation (BEDA)

At leading order in QCD, the BEDA for a longitudinally boost-invariant expanding plasma of quarks and gluons evolves their distribution function,  $f^a(\mathbf{p}, t)$  as

$$\left( \frac{\partial}{\partial \tau} - \frac{p_z}{\tau} \frac{\partial}{\partial p_z} \right) f^a(\mathbf{p}; t) = C_{2 \leftrightarrow 2}^a[f] + C_{1 \leftrightarrow 2}^a[f], \quad , \quad a = \{g, q, \bar{q}\}. \quad (1)$$

The derivative in the longitudinal momentum,  $p_z$ , is in charge of the longitudinal expansion and the two terms in the right-hand side of the equation are the collision kernels. We can study the thermalization following the time evolution of different macroscopic quantities [5, 6], such as the screening mass squared,  $m_D^2$ , the jet quenching parameter  $\hat{q}$ , the effective temperature  $T_*$  and the effective quark chemical potential,  $\mu_*$ .

In general cases, there is one different value of  $\mu_*$  for each of the quark flavors that participate in the evolution. Nevertheless, in this work we will initialize the system with an overoccupied distribution of gluons, without any fermions. Accordingly, the number of quarks and antiquarks will always be the same and the effective chemical potential will be zero.

### 2.1 The $2 \leftrightarrow 2$ collision kernel

When the diffusion approximation is applied, the  $2 \leftrightarrow 2$  collision kernel can be rewritten as a Fokker-Planck equation plus a source term,  $\mathcal{S}_a$ , [7, 8]

$$C_{2 \leftrightarrow 2}^a = \frac{1}{4} \hat{q}_a(t) \nabla_{\mathbf{p}} \cdot \left[ \nabla_{\mathbf{p}} f^a + \frac{\mathbf{v}}{T_*(t)} f^a (1 + \epsilon_a f^a) \right] + \mathcal{S}_a \equiv \left( \text{diagram 1} \right) + \left( \text{diagram 2} \right) \quad (2)$$

$$S_q = \frac{2\pi\alpha_s^2 C_F^2 \mathcal{L}}{p} \left[ I_c f(1-F) - \bar{I}_c F(1+f) \right], \quad S_{\bar{q}} = S_q|_{F \leftrightarrow \bar{F}}, \quad S_g = -\frac{N_f}{2C_F} (S_q + S_{\bar{q}}). \quad (3)$$

Here, we have renamed  $f^g \equiv f$ ,  $f^q \equiv F$  and  $f^{\bar{q}} \equiv \bar{F}$  by convenience and  $\epsilon_a$  is the sign associated with the statistics of species  $a$ . Also, the logarithm  $\mathcal{L} \equiv \ln \frac{\langle p_T^2 \rangle}{m_D^2}$  has been introduced, and  $\hat{q}_a \equiv C_a$ , with  $C_a$  the Casimir for the color group representation of the particle  $a$ . The quantities  $I_c$  and  $\bar{I}_c$  are integrals of a combination of the distribution functions which relates with the quark chemical potential [6] as  $\mu_* \equiv T_* \ln \frac{I_c}{\bar{I}_c}$ .

If the  $2 \leftrightarrow 2$  kernel is the only term included in Eq. (1) some divergence appears in the infrared at some early times if the system is overoccupied. This feature has been interpreted as the onset of Bose-Einstein Condensate [9]. Its presence can be studied numerically if one applies the correct boundary conditions to the solution [8] by defining a number density of the BEC  $\dot{n}_c \propto \lim_{p \rightarrow 0} p f - T_*$ .

## 2.2 The $1 \leftrightarrow 2$ collision kernel

The  $1 \leftrightarrow 2$  collision kernel in Eq. (1) is computed in the deep LPM regime [10, 11]. Since the splitting described in this regime is collinear, the shape of this collision kernel is the same as that used in the homogenous scenario [6]

$$C_{1 \leftrightarrow 2}^a = \int_0^1 \frac{dx}{x^3} \sum_{b,c} \left[ \frac{\nu_c}{\nu_a} C_{ab}^c(\mathbf{p}/x; \mathbf{p}, \mathbf{p}(1-x)/x) - \frac{1}{2} C_{bc}^a(\mathbf{p}; x\mathbf{p}, (1-x)\mathbf{p}) \right]. \quad (4)$$

In this expression, the sum over the particles  $b$  and  $c$  is such that only the processes given by the QCD interaction vertex appear. The  $\nu_i$  factors are the color and spin degrees of freedom of the particle  $i$ .

## 2.3 The rapid thermalization of the soft sector

Including the  $1 \leftrightarrow 2$  collision kernel in the calculation does not allow the BEC to form. This is because it is more divergent than the  $2 \leftrightarrow 2$  in the infrared and dominates the system behavior in this region of the momentum phase space. The  $1 \leftrightarrow 2$  process forces the system to thermalize due to the detailed balance between the splitting and the merging of gluons in the soft sector.

The same argument applies to the quark production, where the  $g \rightarrow q\bar{q}$  splitting is the dominant contribution. For both cases, we can compute the analytical shape of the function distributions at early times, and verify that they correspond to the behavior of a thermal distribution up to some soft momentum scale  $p_s$ .

$$f(p) \approx \frac{T_*(v_z)}{p} \quad \text{for } p \lesssim p_{s,g} \quad (5)$$

$$F(p) \approx \frac{1}{e^{-\frac{\mu_*(v_z)}{T_*(v_z)}} + 1} \quad \text{for } p \lesssim p_{s,q}, \quad (6)$$

where  $T_* \equiv \int dv_z T_*(v_z)$  and  $\mu_* \equiv \int dv_z \mu_*(v_z)$ . The soft momentum scale is different for quarks and gluons, and they are related to their thermal masses,  $m_q \equiv \int dv_z m_q(v_z)$ ,  $m_g \equiv \int dv_z m_g(v_z)$ :

$$p_{s,g} \equiv [m_g^4(v_z) \tau / 2]^{\frac{2}{5}} \hat{q}_A^{\frac{1}{5}} \quad p_{s,q} \equiv [m_q^4(v_z) \tau / 2]^{\frac{2}{5}} \hat{q}_F^{\frac{1}{5}}, \quad (7)$$

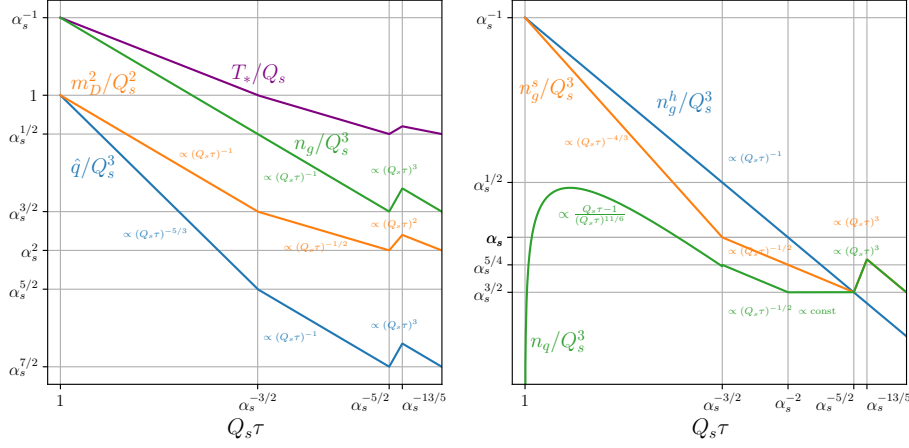


**Figure 1:** Parametric estimates for different macroscopic quantities of the bottom-up thermalization. The left panel shows the effective temperature  $T_*$ , the screening mass squared  $m_D^2$ , the jet quenching parameter  $\hat{q}$ , and the total gluon number density  $n_g$ . The right plot shows the soft and hard gluon number densities,  $n_g^s$  and  $n_g^h$ , as well as the quark number density  $n_q$ .

### 3. Initial conditions and setup

Kinetic theory is a tool exploring the evolution of QCD systems in the weak coupling regime. Therefore, let us assume that  $\alpha_s \ll 1$ . Also, since at early times the system produced by the collision should be mostly given by a highly populated ensemble of soft gluons, we will consider [1] that its function distribution is  $f \sim \alpha_s^{-1}$ . Also, to simplify the calculations, let us assume that the function distribution at the initial time is isotropic in momentum space and characterized by some momentum scale  $Q_s$ .

The isotropy in momentum space will break due to the expansion. Since the expansion is longitudinal and boost invariant [12], the momentum of the partons moving along the transverse direction will not change significantly. That is, their typical momentum will always be  $p_\perp \sim Q_s$ . Nevertheless, any parton that moves along the longitudinal direction ( $v_z \sim 1$ ) will quickly run away from the mid-rapidity region and all the contributions to the typical transverse momentum will be given by the broadening  $p_z \sim \sqrt{\hat{q}\tau}$ . This distinction introduces two characteristic scales to the momentum. We will refer as hard partons to those with typical momentum  $p \sim Q_s$  and soft partons to those with  $p \sim \sqrt{\hat{q}\tau}$ .

### 4. The bottom-up thermalization

In the case of a system composed exclusively of gluons, the parametric behavior is well-known according to Baier, Müller, Schiff and Son [1]. In this section, we extend these parametric estimates by introducing quarks in the calculation and attempt to confirm them by numerical simulations of the BEDA.

We observe that none of the three stages described in [1] are modified, and the three different stages for the thermalization picture persist even after introducing the quark sector in the calculation. These parametrics are shown in Fig. 1. The first stage,  $1 \ll Q_s \tau \ll \alpha_s^{-3/2}$ , is dominated by the

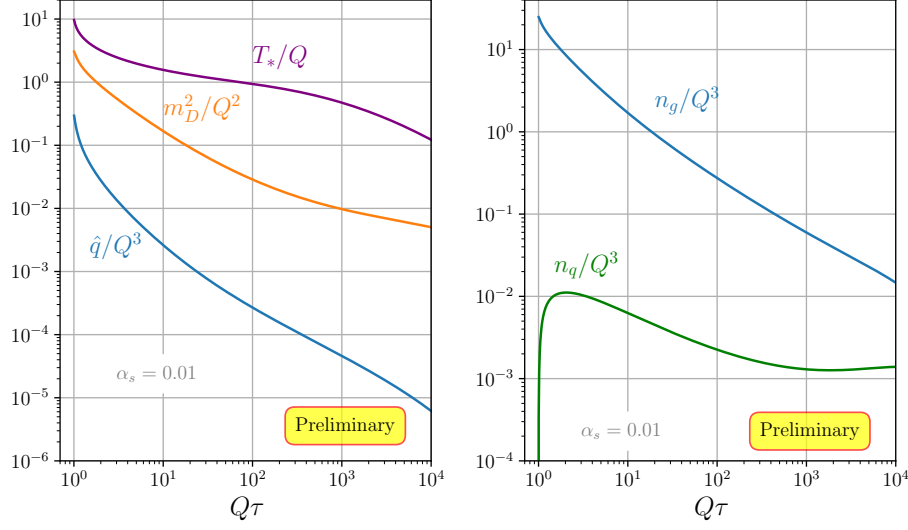


**Figure 2:** Same quantities than those plotted in the simulation shown in Fig. 1, but given by a numerical simulation with  $\alpha_s = 0.01$ .

rapid expansion of hard gluons. In this time region, the soft gluon number density decreases faster than the hard one since for the latter  $n_g \propto p_z^3$ , meanwhile the former follows the Bjorken scaling  $n_g^h \propto (Q_s \tau)^{-1}$ . Also, during this stage, the  $g \rightarrow q\bar{q}$  splitting increases the quark/antiquark number density rapidly until it reaches its higher value and decreases due to the expansion.

The second stage,  $\alpha_s^{-\frac{3}{2}} \ll Q_s \tau \ll \alpha_s^{-\frac{5}{2}}$ , starts at the time that the screening mass is dominated by the soft sector of gluons, even though the number density of hard gluons is still the larger one. This stage ends when these two number densities match each other. This is possible due to the broadening pushing  $p_z$  to a constant value, which slows down the decrease in the soft gluon number density. Similar behavior can be observed for the quark number density up to  $Q_s \tau \sim \alpha_s^{-2}$ . At this time the soft gluon sector starts to dominate the quark production via both  $g \rightarrow q\bar{q}$  and  $gg \rightarrow q\bar{q}$  processes, which are fast enough to counteract the expansion and keep  $n_q$  constant until the parametric matches the gluon number density.

Finally, the third stage,  $\alpha_s^{-\frac{5}{2}} \ll Q_s \tau \ll \alpha_s^{-\frac{13}{5}}$ , corresponds to the thermalization of the soft sector. Up to this point, the majority of the quarks and gluons of the system are soft and have established thermal equilibrium among themselves. The remaining hard gluons will radiate their energy, depositing it into the soft thermal bath and producing the reheating of this thermalized QGP.

#### 4.1 Numerical simulations

Numerical simulations that partially confirm this parametric behavior are plotted in Fig. 2. Here one can see how the macroscopic quantities decrease according to the expansion. Also, observing how the quark number density exhibits the predicted constant behavior is qualitatively possible. Nevertheless, no reheating is observed. This is because this stage is expected to happen at  $Q_s \tau \sim \alpha_s^{-\frac{5}{2}} = 10^5$ , and due to technical reasons we were not able to continue further with the simulation.

## 5. Conclusions and outlook

We have shown that the BEDA is a tool for exploring the evolution of the thermalization process that happens during the initial stages of a heavy ion collision. The BMSS parametric estimates have been extended by allowing the system to produce quarks during the evolution, which do not affect the overall evolution of the system. This parametric estimate has been partially and qualitatively confirmed by comparison with a numerical simulation of the BEDA. The last stage of the parametric remains unclear and finer simulations need to be performed in the future to elucidate if the reheating appears right before the thermalization.

## References

- [1] R. Baier, A.H. Mueller, D. Schiff and D.T. Son, 'Bottom up' thermalization in heavy ion collisions, *Phys. Lett. B* **502** (2001) 51 [[hep-ph/0009237](#)].
- [2] P.B. Arnold, G.D. Moore and L.G. Yaffe, *Effective kinetic theory for high temperature gauge theories*, *JHEP* **01** (2003) 030 [[hep-ph/0209353](#)].
- [3] A. Kurkela and E. Lu, *Approach to Equilibrium in Weakly Coupled Non-Abelian Plasmas*, *Phys. Rev. Lett.* **113** (2014) 182301 [[1405.6318](#)].
- [4] X. Du and S. Schlichting, *Equilibration of weakly coupled QCD plasmas*, *Phys. Rev. D* **104** (2021) 054011 [[2012.09079](#)].
- [5] S.B. Cabodevila, C.A. Salgado and B. Wu, *Thermalization of gluons in spatially homogeneous systems*, *Physics Letters B* **834** (2022) 137491.
- [6] S.B. Cabodevila, C.A. Salgado and B. Wu, *Quark production and thermalization of the quark-gluon plasma*, *JHEP* **06** (2024) 145 [[2311.07450](#)].
- [7] A.H. Mueller, *Toward equilibration in the early stages after a high-energy heavy ion collision*, *Nucl. Phys. B* **572** (2000) 227 [[hep-ph/9906322](#)].
- [8] J.-P. Blaizot, B. Wu and L. Yan, *Quark production, Bose-Einstein condensates and thermalization of the quark-gluon plasma*, *Nucl. Phys. A* **930** (2014) 139 [[1402.5049](#)].
- [9] J.-P. Blaizot, J. Liao and L. McLerran, *Gluon Transport Equation in the Small Angle Approximation and the Onset of Bose-Einstein Condensation*, *Nucl. Phys. A* **920** (2013) 58 [[1305.2119](#)].
- [10] R. Baier, Y.L. Dokshitzer, A.H. Mueller, S. Peigne and D. Schiff, *Radiative energy loss of high-energy quarks and gluons in a finite volume quark - gluon plasma*, *Nucl. Phys. B* **483** (1997) 291 [[hep-ph/9607355](#)].
- [11] P.B. Arnold and C. Dogan, *QCD Splitting/Joining Functions at Finite Temperature in the Deep LPM Regime*, *Phys. Rev. D* **78** (2008) 065008 [[0804.3359](#)].
- [12] J.D. Bjorken, *Highly relativistic nucleus-nucleus collisions: The central rapidity region*, *Phys. Rev. D* **27** (1983) 140.